Oxidation of $CpM(CO)_3^{\bullet}$ and $CpM(CO)_3(NCMe)^{\bullet}$ (M = Cr, Mo, W): Kinetic and Thermodynamic Considerations of Their Possible Involvement as Reducing Agents. Relative Acetonitrile Affinities of $CpM(CO)_3^{+}$ and $CpM(CO)_3^{\bullet}$

Mats Tilset[1]

Department of Chemistry, University of Oslo, P.O. Box 1033 Blindern, N-0315 Oslo, Norway

Received March 3, 1994[⊗]

The electrochemistry of the anions, radicals, and cations $CpM(CO)_3^{-/\bullet/+}$ (M = Cr, Mo, W) in acetonitrile has been reinvestigated by cyclic voltammetry and digital simulation techniques. For M = Cr, oxidation of the persistent radical to the cation is directly observed at a potential ca. 1.0 V more positive than the anion oxidation potential. For M = Mo and W, oxidation of the 17-electron radicals cannot be directly observed due to the rapid follow-up dimerization reactions. Thermochemical considerations establish that the generation of the cationic products $CpM(CO)_3(NCMe)^{+}$ (M = Mo, W) even at the anion oxidation potentials cannot be due to the direct oxidation of the radicals $CpM(CO)_3^{\bullet}$. Digital simulation results demonstrate that the 19-electron radicals $CpM(CO)_3(NCMe)^{\bullet}$, which are stronger reducing agents than $CpM(CO)_3^{\bullet}$ by about 1.4 V, are kinetically and thermodynamically competent intermediates for the production of the cations by heterogeneous and homogeneous electron transfer. A thermochemical cycle shows that acetonitrile binds more strongly to the 16-electron cations $CpM(CO)_3^{+}$ than to the 17-electron radicals $CpM(CO)_3^{\bullet}$ by ca. 135 kJ/mol.

Introduction

The chemistry of 17- and 19-electron organotransition-metal radicals has been vigorously investigated during the last decade.[2] The group 6 radicals $CpM(CO)_3^{\bullet}$ (M = Cr, Mo, W) and substituted derivatives arguably are some of the most intensely studied neutral organometal radicals. The Mo- and W-centered radicals are commonly produced by photochemical homolysis[3] of the metal–metal-bonded dimers (eq 1) and have been seen to engage in atom abstraction[3c,4] and in the frequently coupled ligand substitution and disproportionation[5] reactions.

$$[CpM(CO)_3]_2 \longrightarrow 2\,CpM(CO)_3^{\bullet} \quad (1)$$

$$CpM(CO)_3^{-} \longrightarrow CpM(CO)_3^{\bullet} + e^{-} \quad (2)$$

The chemical or electrochemical oxidation of metal anions represents another commonplace method for the generation of the radicals (eq 2).[6] Dessy and co-workers[6a] found that $[CpMo(CO)_3]_2$ undergoes a chemically irreversible reduction to give $CpMo(CO)_3^{-}$. When oxidized, the anion yielded $CpMo(CO)_3^{\bullet}$, which rapidly reacted with the Hg electrode to yield $[CpMo(CO)_3]_2Hg$. The anion oxidation proceeds irreversibly also at the Pt electrode, and this has been attributed primarily to radical dimerization which produces $[CpM(CO)_3]_2$ (M = Mo, W).[6c,f] For M = Cr, the dimer exists in equilibrium with the monomeric radical in solution[7a] due to the rather weak Cr–Cr bond in the dimer; substituted analogs have even weaker Cr–Cr bonds and in some cases exist as monomers (radicals) in solution and in the solid state.[7b-i] As a consequence, the oxidation of the Cr-centered anions proceeds reversibly to give quite persistent radicals.[7a,e,g,h]

In 1986,[6c] Kadish and co-workers noted that the cyclic voltammograms of the anions $CpM(CO)_3^{-}$ (M = Mo, W) revealed that not only were the dimers formed during the anion oxidation but also the cationic species $CpM(CO)_3(Sol)^{+}$ (Sol = MeCN, THF, dichloromethane) were formed. Significantly, the cations were produced at potentials that should not lead to oxidation of the dimers. This observation was interpreted as an indication that the radicals $CpM(CO)_3^{\bullet}$ are oxidized at the electrode potential where the anions $CpM(CO)_3^{-}$ are oxidized. Such an event would indeed be rather surprising, since intuitively the electron-deficient 17-electron radical should be more resistant toward oxidation than the electron-rich 18-electron anion. This

⊗ Abstract published in *Advance ACS Abstracts*, June 1, 1994.

(1) E-mail: MATS.TILSET@KJEMI.UIO.NO.

(2) (a) Geiger, W. E. *Prog. Inorg. Chem.* **1985**, *33*, 275. (b) Kochi, J. K. *J. Organomet. Chem.* **1986**, *300*, 139. (c) Stiegman, A. E.; Tyler, D. R. *Comments Inorg. Chem.* **1986**, *5*, 215. (d) Tyler, D. R. *Prog. Inorg. Chem.* **1988**, *36*, 125. (e) Astruc, D. *Chem. Rev.* **1988**, *88*, 1189. (f) Baird, M. C. *Chem. Rev.* **1988**, *88*, 1217. (g) Connelly, N. G. *Chem. Soc. Rev.* **1989**, *18*, 153. (h) *Paramagnetic Organometallic Species in Activation/Selectivity, Catalysis*; Chanon, M., Julliard, M., Poite, J. C., Eds.; Kluwer Academic: Dordrecht, The Netherlands, 1989. (i) Tyler, D. R.; Mao, F. *Coord. Chem. Rev.* **1990**, *97*, 119. (j) *Organometallic Radical Processes*; Trogler, W. C., Ed.; Elsevier: Amsterdam, 1990. (k) Astruc, D. *Acc. Chem. Res.* **1991**, *24*, 36. (l) Tyler, D. R. *Acc. Chem. Res.* **1991**, *24*, 325.

(3) (a) Hughey, J. L.; Bock, C. R.; Meyer, T. J. *J. Am. Chem. Soc.* **1975**, *97*, 4440. (b) Geoffroy, G. L.; Wrighton, M. S. *Organometallic Photochemistry*; Academic Press: New York, 1979. (c) Hepp, A. F.; Wrighton, M. S. *J. Am. Chem. Soc.* **1981**, *103*, 1258. (d) Meyer, T. J.; Caspar, J. V. *Chem. Rev.* **1985**, *85*, 187. (e) Scott, S. L.; Espenson, J. H.; Zhu, Z. *J. Am. Chem. Soc.* **1993**, *115*, 1789.

(4) For recent reviews, see: (a) Brown, T. L.; Sullivan, R. J. In ref 2h, p 187. (b) Brown, T. L. In ref 2j, p 67.

(5) For recent reviews, see refs 2c,d,i and: (a) Tyler, D. R.; Philbin, C.; Fei, M. In ref 2h, p 201. (b) Trogler, W. C. In ref 2j, p 306. (c) Tyler, D. R. In ref 2j, p 338.

(6) For key references to some aspects of the electron-transfer chemistry of $CpM(CO)_3^{\bullet}$ (M = Mo, W) and related anions and dimers, see: (a) Dessy, R. E.; Stary, F. E.; King, R. B.; Waldrop, M. *J. Am. Chem. Soc.* **1966**, *88*, 471. (b) Dessy, R. E.; Weissman, P. M.; Pohl, R. L. *J. Am. Chem. Soc.* **1966**, *88*, 5117. (c) Kadish, K. M.; Lacombe, D. A.; Anderson, J. E. *Inorg. Chem.* **1986**, *25*, 2246. (d) Ryan, O. B.; Tilset, M.; Parker, V. D. *J. Am. Chem. Soc.* **1990**, *112*, 2618. (e) Corraine, M. S.; Atwood, J. D. *Organometallics* **1991**, *10*, 2315. (f) Pugh, J. R.; Meyer, T. J. *J. Am. Chem. Soc.* **1992**, *114*, 3784. (g) Scott, S. L.; Espenson, J. H.; Chen, W.-J. *Organometallics* **1993**, *12*, 4077.

(7) (a) Madach, T.; Vahrenkamp, H. *Z. Naturforsch.* **1978**, *33B*, 1301. (b) Goh, L.-Y.; D'Aniello, M. J., Jr.; Slater, S.; Muetterties, E. L.; Tavanaiepour, I.; Chang, M. I.; Fredrich, M. F.; Day, V. W. *Inorg. Chem.* **1979**, *18*, 192. (c) Jaeger, T. J.; Baird, M. C. *Organometallics* **1986**, *5*, 2563. (d) Cooley, N. A.; MacConnachie, P. T. F.; Baird, M. C. *Polyhedron* **1988**, *7*, 1965. (e) O'Callaghan, K. A. E.; Brown, S. J.; Page, J. A.; Baird, M. C.; Richards, T. C.; Geiger, W. E. *Organometallics* **1991**, *10*, 3119. (f) Watkins, W. C.; Jaeger, T.; Kidd, C. E.; Fortier, S.; Baird, M. C.; Kiss, G.; Roper, G. C.; Hoff, C. D. *J. Am. Chem. Soc.* **1992**, *114*, 907. (g) Tilset, M. *J. Am. Chem. Soc.* **1992**, *114*, 2740. (h) Hoobler, R. J.; Hutton, M. A.; Dillard, M. M.; Castellani, M. P.; Rheingold, A. L.; Rieger, A. L.; Rieger, P. H.; Richards, T. C.; Geiger, W. E. *Organometallics* **1993**, *12*, 116. (i) Yao, Q.; Bakac, A.; Espenson, J. H. *Organometallics* **1993**, *12*, 2010.

0020-1669/94/1333-3121$04.50/0

is in accord with the notion that "direct", 2-electron-transfer processes usually take place with intervening chemical reactions, including conformational changes or ligand additions, that render the second electron transfer more favorable than the first.[8]

It still remains to be rigorously established whether the electrochemical generation of the solvates $CpM(CO)_3(Sol)^+$ occurs by direct oxidation of the radical followed by rapid capture of the resulting 16-electron cation by the solvent (eq 3) or by prior coordination of a solvent molecule and subsequent oxidation of the more electron-rich 19-electron radical adduct (eq 4). The coordination of 2-electron donors at neutral 17-electron radicals has been shown to produce highly reducing 19-electron radicals.[5b,c,21]

$$CpM(CO)_3^{\bullet} \xrightarrow{-e^-} CpM(CO)_3^+ \xrightarrow{Sol} CpM(CO)_3(Sol)^+ \quad (3)$$

$$CpM(CO)_3^{\bullet} \xrightarrow{Sol} CpM(CO)_3(Sol)^{\bullet} \xrightarrow{-e^-} CpM(CO)_3(Sol)^+ \quad (4)$$

Hepp and Wrighton[3c] first reported that photogenerated $CpW(CO)_3^{\bullet}$ is able to reduce Cp_2Fe^+ in acetonitrile and other solvents and found that the relative rate of radical oxidation vs atom abstraction was greater in acetonitrile than in dichloromethane. Espenson and co-workers[6g] extended this work in a recent kinetic study in which it was reported that $CpW(CO)_3^{\bullet}$ generated by laser flash photolysis in acetonitrile acted as a reductant toward Cp_2Fe^+ and as an oxidant toward Cp^*_2Fe ($Cp^* = \eta^5$-C_5Me_5). For these *homogeneous* electron-transfer reactions, the question again arises as to what the exact nature of the true reductant toward Cp_2Fe^+ is: Is it $CpW(CO)_3^{\bullet}$ itself, or is it the solvent adduct $CpW(CO)_3(NCMe)^{\bullet}$? On the basis of kinetic arguments, Espenson et al.[6g] convincingly argued that the equilibrium between $CpW(CO)_3^{\bullet}$ and $CpW(CO)_3(NCMe)^{\bullet}$ in acetonitrile must be rather unfavorable. It was still considered kinetically possible that the reactive species which reduced Cp_2Fe^+ was $CpW(CO)_3(NCMe)^{\bullet}$, although the authors favored the alternative direct reduction by $CpW(CO)_3^{\bullet}$. On the other hand, the enhanced rate of reaction between Cp_2Fe^+ and $CpW(CO)_3^{\bullet}$ in the presence of PPh_3 was attributed to the generation of the 19-electron radical $CpW(CO)_3(PPh_3)^{\bullet}$.

In this paper, we take a new look at the electrochemical oxidation of the $CpM(CO)_3^-$ anions (M = Cr, Mo, W) in acetonitrile and dichloromethane. The question regarding the nature of the species being oxidized during the cation generation is addressed specifically. Implications regarding the mechanism of the homogeneous electron-transfer reactions are discussed. The experimental results are obtained by cyclic voltammetry (CV) at moderate voltage sweep rates (v = 0.1–10 V/s). Digital simulations of the electrode processes, made possible by recent important advances in electrochemical simulations, are included to furnish quantitative kinetic data for the discussion.

Results

Oxidation of $CpCr(CO)_3$-PPN$^+$. Figure 1 shows cyclic voltammograms for the oxidation of $CpCr(CO)_3$-PPN$^+$ in acetonitrile/0.1 M $Bu_4N^+PF_6^-$ (d = 0.6 mm Pt disk electrode, 19 °C, voltage sweep rate v = 1.0 V/s). The top trace shows the reversible couple labeled I, II centered at E = –0.68 V vs the Cp_2Fe/Cp_2Fe^+ (Fc) couple. The bottom trace shows a voltammogram which is taken to a more positive potential and which shows a broader, chemically irreversible oxidation wave with a peak potential at 0.42 V vs Fc, labeled III. In addition, an accompanying reduction wave labeled IV is seen with a peak potential at –0.92 V vs Fc during the reverse scan. This wave is not seen in the top trace; nor was any evidence for it seen under the same conditions as used when the top trace was recorded except that the scan rate was lowered to 0.1 V/s.

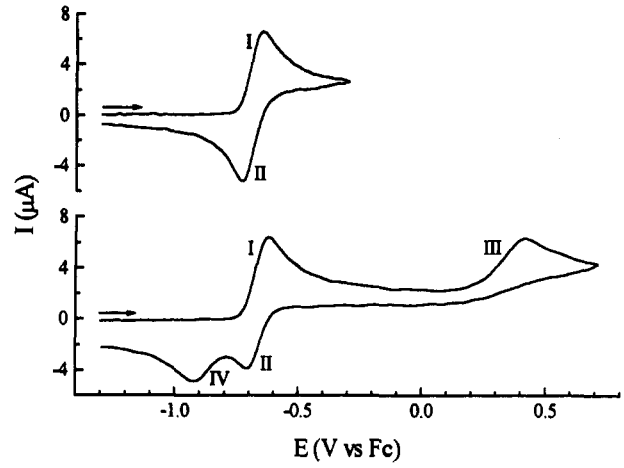

Figure 1. Cyclic voltammograms for the oxidation of $CpCr(CO)_3$-PPN$^+$ in acetonitrile/0.1 M $Bu_4N^+PF_6^-$ (1.0 mM substrate, 0.6 mm diameter Pt disk electrode, voltage sweep rate v = 1.0 V/s, 19 °C).

The I, II peaks can be unambiguously assigned to the $CpCr(CO)_3^{-/\bullet}$ couple. It was discussed recently that the irreversible wave III could be due either to the oxidation of $CpCr(CO)_3^{\bullet}$ to $CpCr(CO)_3^+$ or to the oxidation of $[CpCr(CO)_3]_2$, which is in equilibrium with the monomeric radical in solution.[7e] It is not too important for our discussion whether wave III is caused by dimer or monomer oxidation; it is more important to note that the potential of this wave represents a *minimum value* for the oxidation potential of the monomer. Monomer oxidation yields the electron-deficient 16-electron cation $CpCr(CO)_3^+$, at which the solvent undoubtedly coordinates to yield $CpCr(CO)_3(NCMe)^+$. The wave at IV is caused by the reduction of this cation. This cation has never been isolated but has been previously generated by the 2-electron oxidation of $CpCr(CO)_3H$.[6d] The IR ν_{CO} absorptions of the cation closely match those of the Mo and W congeners, and its reduction potential is more negative than that of $CpCr(CO)_3^{\bullet}$, in analogy with the behavior of the Mo and W counterparts. In support of the notion that wave III may be caused by monomer oxidation, we note that $TpM(CO)_3^{\bullet}$ and $Tp'M(CO)_3^{\bullet}$[9] (M = Cr, Mo, W), which exist as radicals even in the solid state,[10] undergo oxidation at potentials 0.8–0.9 V more positive than the corresponding anion oxidations.[10de,11]

Two important conclusions may be drawn from this part of the work: (1) $CpCr(CO)_3^{\bullet}$ is more difficult to oxidize than $CpCr(CO)_3^-$ by at least 1.1 V, disregarding non-Nernstian behavior and kinetic potential shifts that contribute to the position of wave III; (2) $CpCr(CO)_3(NCMe)^+$ is generated only when the CV experiment encompasses wave III. *The cation $CpCr(CO)_3(NCMe)^+$ is not produced at the oxidation potential of the anion $CpCr(CO)_3^-$.*

Oxidation of $CpMo(CO)_3$-PPN$^+$ and $CpW(CO)_3$-PPN$^+$ in Acetonitrile. Figure 2 shows cyclic voltammograms for the oxidation of $CpMo(CO)_3$-PPN$^+$ and $CpW(CO)_3$-PPN$^+$ under the same conditions as those employed for the oxidation of $CpCr(CO)_3$-PPN$^+$ in Figure 1. The peak potentials for the oxidation of both anions are practically identical at 0.48 V vs Fc. The radicals that are produced undergo dimerization at rates near diffusion control[3e] (3.9×10^9 and 6.2×10^9 M^{-1} s^{-1} for

(8) (a) Richardson, D. E.; Taube, H. *Coord. Chem. Rev.* **1984**, *60*, 107. (b) Astruc, D.; Lacoste, M.; Toupet, L. *J. Chem. Soc., Chem. Commun.* **1990**, 558.

(9) Tp = hydrotris(pyrazolyl)borate; Tp' = hydrotris(3,5-dimethylpyrazolyl)-borate.

(10) (a) Curtis, M. D.; Shiu, K.-B.; Butler, W. M.; Huffman, J. C. *J. Am. Chem. Soc.* **1986**, *108*, 3335. (b) Shiu, K.-B.; Lee, L.-Y. *J. Organomet. Chem.* **1988**, *348*, 357. (c) MacNeil, J. H.; Watkins, W. C.; Baird, M. C.; Preston, K. F. *Organometallics* **1992**, *11*, 2761. (d) Bockman, T. M.; Kochi, J. K. *New J. Chem.* **1992**, *16*, 39. (e) Protasiewicz, J. D.; Theopold, K. H. *J. Am. Chem. Soc.* **1992**, *115*, 5559.

(11) Skagestad, V.; Tilset, M. *J. Am. Chem. Soc.* **1993**, *115*, 5077.

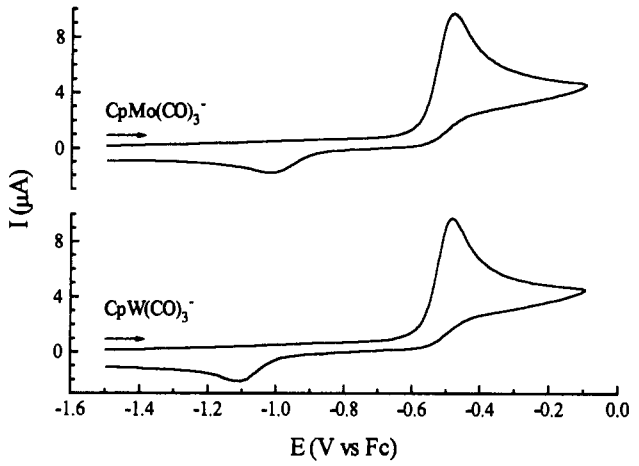

Figure 2. Cyclic voltammograms for the oxidation of $CpMo(CO)_3^-PPN^+$ (top) and $CpW(CO)_3^-PPN^+$ (bottom) in acetonitrile/0.1 M $Bu_4N^+PF_6^-$ (1.0 mM substrate, 0.6 mm diameter Pt disk electrode, voltage sweep rate v = 1.0 V/s, 19 °C).

Mo and W, respectively, in acetonitrile), and this causes the waves to be chemically irreversible and subject to cathodic kinetic potential shifts of slightly more than 0.1 V, assuming a Nernstian electron transfer.[12] During the cathodic scans, both voltammograms show that product peaks at −1.0 and −1.1 V vs Fc, respectively, are formed. These waves are caused by the reduction of $CpMo(CO)_3(NCMe)^+$ and $CpW(CO)_3(NCMe)^+$, verified by running cyclic voltammograms of authentic samples of their PF_6^- salts. The waves due to reduction of the dimers $[CpM(CO)_3]_2$ were seen at potentials more negative than those shown in the figures. This is in agreement with previous studies.[6c,f]

At more positive potentials (not shown here), another irreversible oxidation wave was seen for both metals. These waves have been attributed to the irreversible oxidation of the dimers.[6c] Since dimer formation from the radicals is extremely fast and irreversible for the Mo and W species, the radicals have insufficient lifetime to be detected on the relatively slow time scale of our CV experiments and therefore we also consider that this assignment of the second oxidation waves is unambiguous.

For our purpose, the most important observation in these experiments is that *the cations $CpM(CO)_3(NCMe)^+$ (M = Mo, W) are generated at the potentials at which the anions are oxidized.* This behavior is in obvious contrast to the results obtained for the Cr analogue.

Oxidation of $CpMo(CO)_3^-PPN^+$ in Dichloromethane. Figure 3 shows a cyclic voltammogram for the oxidation of $CpMo(CO)_3^-PPN^+$ in dichloromethane/0.2 M $Bu_4N^+PF_6^-$ but otherwise under identical conditions to those used above. The oxidation peak potential has been shifted ca. 0.1 V to more negative values in the new solvent. The direction of the shift is as might be expected because the reduced state (anion) is more stabilized by solvation in the more polar solvent acetonitrile for the substrate, whereas it is the oxidized state that is more stabilized in the polar solvent for the ferrocene reference couple. The oxidation of $CpMo(CO)_3^-$ is still irreversible. The wave that begins at the end of the reverse scan is caused by onset of reduction of the dimer, which is produced by radical dimerization. Importantly, during the reverse scan there is no evidence for the generation of any cationic products that are reducible. This contrasts with Kadish's finding[6c] that, even in dichloromethane, a cation was detected which was assumed to be the solvate and which was reduced at a potential ca. 0.3 V more negative than the anion oxidation wave. In that study, $Bu_4N^+ClO_4^-$ was used as the supporting electrolyte. Since ClO_4^- is a more potent ligand than PF_6^-, we surmise that the reduction wave was caused by a

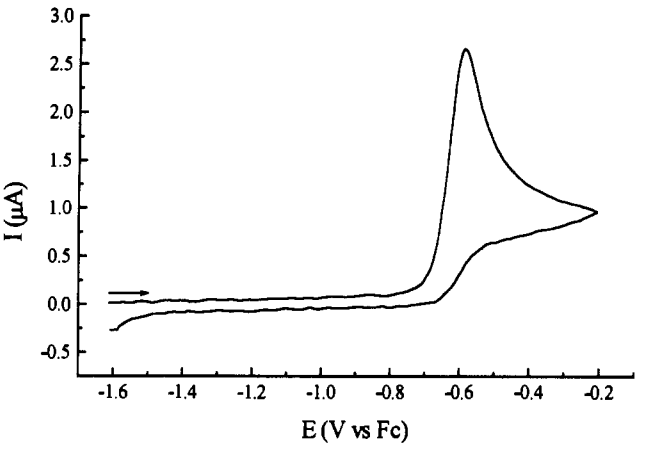

Figure 3. Cyclic voltammogram for the oxidation of $CpMo(CO)_3^-PPN^+$ in dichloromethane/0.2 M $Bu_4N^+PF_6^-$ (1.0 mM substrate, 0.6 mm diameter Pt disk electrode, voltage sweep rate v = 1.0 V/s, 19 °C).

perchlorate, rather than a dichloromethane, adduct. The tendency of ClO_4^- to coordinate at 17-electron cations even when the reasonably good ligand acetone is employed as the solvent[13a] and to lead to reduced chemical reversibility when compared with PF_6^- in voltammetric experiments[13b] has been demonstrated. In conclusion, our experiments show that *no* dichloromethane adduct is detectable. The same result was obtained for the oxidation of $CpW(CO)_3^-$.

Digital Simulation of the Cyclic Voltammetry Response for the Oxidation of $CpMo(CO)_3^-$. Digital simulation techniques have proven of utmost value for the modeling of electron-transfer reactions at electrode surfaces.[14a,b] Simulation often is the only way to theoretically predict the I vs E response for electron-transfer reactions coupled by homogeneous reactions. The explicit finite difference algorithm, applied to cyclic voltammetry by Feldberg in 1969,[14c] has been particularly attractive, in part because it is easily understood and programmed. However, a serious limitation is met when k/v is large, i.e. when the homogeneous reactions are very fast relative to the voltage sweep rates, because the number of iterations required will be immense. These problems were overcome by a recent development in digital simulations. The program DIGISIM,[15a] described recently by Rudolph, Reddy, and Feldberg,[15b] uses a fast implicit finite difference algorithm rather than explicit methods for solving the complex differential equations. As a result, even the fastest reactions can now be simulated in a few seconds on a desktop personal computer. Digital simulations were performed, and the correspondence between experimental and simulated data were optimized, with the DIGISIM program.

At the beginning of the Results, we demonstrated that $CpCr(CO)_3^{\bullet}$ is more difficult to oxidize than $CpCr(CO)_3^-$ by ca. 1 V. It is reasonable (see also the Discussion) that the same applies to the Mo and W analogues. Consequently, in CV experiments where the switching potential is located well in advance of the second oxidation wave (as for Figure 1, top) the 17-electron radical will not be oxidized to any extent that will generate detectable amounts of the cation $CpM(CO)_3(NCMe)^+$ on the reverse scan. This was substantiated by digital simulations of the process depicted in Scheme 1. It proved impossible to reproduce voltammograms similar to those in Figure 2 on the basis of this

(12) Bard, A. J.; Faulkner, L. R. *Electrochemical Methods: Fundamentals and Applications*, Wiley: New York, 1980; p 454.

(13) (a) Liu, H.-Y.; Golovin, M. N.; Fertal, D. A.; Tracey, A. A.; Eriks, K.; Giering, W. P.; Prock, A. *Organometallics* **1989**, *8*, 1454. (b) Stone, N. J.; Sweigart, D. A.; Bond, A. M. *Organometallics* **1986**, *5*, 2553.

(14) (a) Reference 12, p 675. (b) Gosser, D. K., Jr. *Cyclic Voltammetry: Simulation and Analysis of Reaction Mechanisms*; VCH: Weinheim, Germany, 1993. (c) Feldberg, S. W. In *Electroanalytical Chemistry*; Bard, A. J., Ed.; Marcel Dekker: New York, 1969; Vol. 3, p 199.

(15) (a) Trademark of Bioanalytical Systems Inc., W. Lafayette, IN. (b) Rudolph, M.; Reddy, D. P.; Feldberg, S. W. *Anal. Chem.*, submitted for publication.

Scheme 1

$$CpM(CO)_3^- \overset{E_{anion}}{\rightleftharpoons} CpM(CO)_3^{\bullet} + e^-$$

$$CpM(CO)_3^{\bullet} \overset{E_{radical}}{\rightleftharpoons} CpM(CO)_3^+ + e^-$$

$$CpM(CO)_3^+ + MeCN \longrightarrow CpM(CO)_3(NCMe)^+$$

$$CpM(CO)_3^{\bullet} \longrightarrow 0.5\ Cp_2M_2(CO)_6$$

Scheme 2

$$CpM(CO)_3^- \overset{E_5}{\rightleftharpoons} CpM(CO)_3^{\bullet} + e^- \quad (5)$$

$$CpM(CO)_3^{\bullet} + MeCN \underset{k_{-6}}{\overset{k_6}{\rightleftharpoons}} CpM(CO)_3(NCMe)^{\bullet} \quad (6)$$

$$CpM(CO)_3(NCMe)^{\bullet} \overset{E_7}{\rightleftharpoons} CpM(CO)_3(NCMe)^+ + e^- \quad (7)$$

$$CpM(CO)_3^{\bullet} \xrightarrow{k_8} 0.5\ Cp_2M_2(CO)_6 \quad (8)$$

$$CpM(CO)_3^{\bullet} + CpM(CO)_3(NCMe)^{\bullet} \underset{k_{-9}}{\overset{k_9}{\rightleftharpoons}} CpM(CO)_3^- + CpM(CO)_3(NCMe)^+ \quad (9)$$

scheme using reasonable values for $E_{radical} - E_{anion}$ (0.5 V or more). Peak IV could under no circumstances be reproduced in the simulated voltammograms—not even if the second electrode process was assumed to be a Nernstian electron transfer that was driven by diffusion-controlled trapping of $CpM(CO)_3^+$ by the solvent acetonitrile.

On the other hand, successful simulations based on Scheme 2 were readily achieved. Obviously, a great number of adjustable parameters are involved. In addition to the kinetic parameters for the homogeneous reactions, the electrode potentials E, the transfer coefficients α, and the heterogeneous electron transfer rate constants k_s for reactions 5 and 7 must be taken into account. The CV behavior of the anions was excellent, but even with the little extent of experimental variations (see Experimental Section for details) it would be meaningless to claim high accuracy for each parameter in an optimization process. Not surprisingly, the work established that a range of choices for most parameters could result in acceptable fits between experimental and simulated data.

The major goal of doing the simulations was to establish values for the equilibrium and rate constants for reversible reaction 6. Fortunately, the optimized values for k_6 and k_{-6} were not highly dependent on the exact value of the other parameters. This finding reflects that it is the relative rate of reaction 6 compared to the dimerization reaction 8 that is the most important factor for deciding the intensity of peak IV on the reverse scan. Thus, fixing the values for α and k_s for reactions 5 and 7 at values quite different from the optimized values in Table 1 (as long as grossly distorted voltammograms did not result) affected the optimized values for the rate constants pertaining to reaction 6 by less than 20–30%.

Espenson and co-workers recently reported[3e] a rate constant $k_8 = 3.9 \times 10^9\ M^{-1}\ s^{-1}$ for the dimerization of $CpMo(CO)_3^{\bullet}$ in acetonitrile, obtained from photochemical experiments, and this value has been used in all simulations. The highly exergonic cross-electron-transfer reaction 9 was included in the simulation model. Equilibrium constant K_9 is defined by E_5 and E_7 through the Nernst equation. The forward reaction rate must be limited by diffusion control; i.e. $k_9 < 3 \times 10^{10}\ M^{-1}\ s^{-1}$.[3e] Variations in k_9 while other parameters (except those pertaining to eq 6) were kept constant had no significant (<10%) effect on the optimized k_6 values when k_9 was adjusted from diffusion control to $10^8\ M^{-1}\ s^{-1}$. The reason for this is that an unfavorable equilibrium 6 renders reaction 9 slow in comparison with the radical dimerization even for a diffusion-controlled reaction 9. This means that the generation of $CpMo(CO)_3(NCMe)^+$ in essence takes place only at the electrode surface and not in solution by eq 9.

In the simulations, diffusion coefficients for all electroactive species were taken to be $10^{-5}\ cm^2\ s^{-1}$. A dimensionless equilibrium constant $K'_6 = K_6[MeCN] = k_6[MeCN]/k_{-6}$ was used for input in the simulations; K'_6 simply equals the equilibrium $[CpM(CO)_3(NCMe)^{\bullet}]/[CpM(CO)_3^{\bullet}]$ ratio. The value for K'_6 was systematically varied from 10^{-2} to 10^{-5}. Values lower than ca. 10^{-5} require reverse reaction 9 to proceed faster than typical bond vibrations (vide infra) and were not used. For each value of K'_6, the values of the pseudo-first-order forward rate constant for eq 6, $k'_6 = k_6[MeCN]$, and E, α, and k_s for reactions 5 and 7 were optimized by the iterative procedure included in DIGISIM. First, separate optimizations were performed for each of the two peaks I and IV of the voltammogram. The values for E_5, α_5, and k_{s5} did not depend on the corresponding values for reaction 7, and essentially identical values were obtained for all simulations.[16] Then, the results of the two separate optimizations were used as input for a full iterative optimization. As mentioned earlier, we are fully aware that a great deal of uncertainty is involved for some parameters. However, the important thing to note is that the optimized values for k_6 were not sensitive to the exact value of these parameters. For $K'_6 = 10^{-3}$, the best fit assuming $\alpha = 0.5$ and Nernstian behavior for both electrode processes was not good but the best value for k_6 deviated only by 50% from the value in Table 1. Even a deviation of this magnitude will not affect any of the qualitative conclusions that may be drawn from this work.

Table 1. Digital Simulation Data for the CV Response for the Oxidation of $CpMo(CO)_3^-$ at $v = 1.0\ V/s$[a]

K'_6	k'_6 (s^{-1})	K_6[b] (M^{-1})	k_6[c] ($M^{-1}\ s^{-1}$)	k_{-6} (s^{-1})	E_7 (V vs FC)	k_{s7} ($cm\ s^{-1}$)	α_7
10^{-2}	6.3×10^5	5.6×10^{-4}	3.5×10^4	6.3×10^7	−0.983	0.012	0.69
10^{-3}	6.1×10^6	5.6×10^{-5}	3.4×10^5	6.2×10^9	−1.037	0.050	0.67
10^{-4}	6.0×10^7	5.6×10^{-6}	3.3×10^6	6.0×10^{11}	−1.086	0.17	0.65
10^{-5}	6.0×10^8	5.6×10^{-7}	3.3×10^7	6.0×10^{13}	−1.147	0.83	0.65

[a] $k_8 = 3.9 \times 10^9\ M^{-1}\ s^{-1}$,[3e] $E_7 = -0.489$ V vs Fc, $\alpha_5 = 0.20$, and $k_{s5} = 0.029\ cm\ s^{-1}$ for all simulations. [b] $K_6 = K'_6/[MeCN]$. [c] $k_6 = k'_6/[MeCN]$.

Good agreements between simulated and experimental voltammograms were obtained for a range of K'_6 spanning from 10^{-2} to 10^{-5}. Table 1 summarizes the digital simulation data for $CpMo(CO)_3^-$. For a given value of K'_6, the optimized value for k_6 never deviated by more than 20–30% from the values in Table 1 when the less important parameters were adjusted. Moreover, the parameters in Table 1 led to good agreement with the CV response for measurements performed at $v = 0.1$ and 10 V/s but with otherwise identical conditions. The variable sweep rate voltammograms did not serve to further narrow the range of possible K'_6 or k'_6 values.

Table 1 shows that, in the range $10^{-5} < K'_6 < 10^{-2}$, the product k_6K_6 at best-fit conditions was essentially constant at $18\ M^{-2}\ s^{-1}$. In other words, k_6 and K_6 are inversely related; a small value for K_6 requires k_6 to be large in order for sufficient quantities of the cation $CpM(CO)_3(NCMe)^+$ to be generated at the electrode for detection during the reverse scan. A similar pattern was seen when the voltammograms for $CpW(CO)_3^-$ were simulated. In this case, k_6K_6 was constant at $25\ M^{-2}\ s^{-1}$ for $10^{-2} < K'_6 < 10^{-5}$.

For Mo, the optimized values for k_6 range from $3.5 \times 10^4\ M^{-1}\ s^{-1}$ for $K'_6 = 10^{-2}$ to $3.3 \times 10^7\ M^{-1}\ s^{-1}$ for $K'_6 = 10^{-5}$, approximating the activity of acetonitrile a_{MeCN} as [MeCN] =

(16) (a) The optimized E, α, and k_s values in combination have the effect that the peak potential for the oxidation of $CpMo(CO)_3^-$ coincides with the reversible potential; i.e., the kinetic potential shift is nearly offset by the distortions caused by α being different from 0.5 and the slightly non-Nernstian behavior caused by the small k_s value. In a previous paper dealing with estimating M–H bond energies from thermochemical cycles on the basis of electrochemical data, Nernstian behavior was assumed when a kinetic potential shift was used to arrive at the reversible E value for metal anion oxidations.[16b] The simulation data (this work) leads to E values ca. 90 mV more negative than previously reported for oxidation of $CpMo(CO)_3^-$ and $CpW(CO)_3^-$. As a consequence, the homolytic bond dissociation energies that were reported[16b] for $CpMo(CO)_3H$ and $CpW(CO)_3H$ may have been overestimated by nearly 8 kJ/mol. (b) Parker, V. D.; Handoo, K. L.; Roness, F.; Tilset, M. *J. Am. Chem. Soc.* **1991**, *113*, 7493.

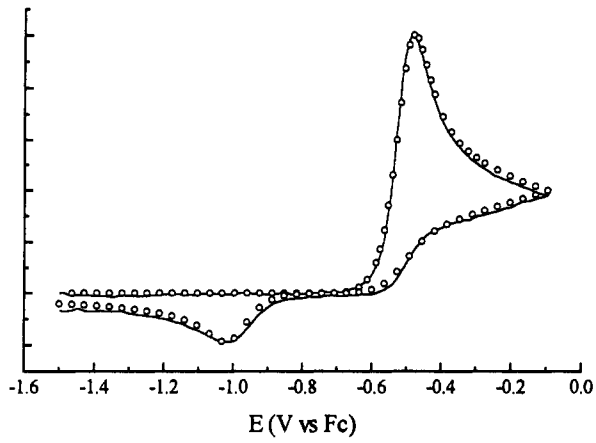

Figure 4. Simulated (circles) and background-subtracted experimental (line) cyclic voltammograms for the oxidation of $CpMo(CO)_3^-$ in acetonitrile. The simulation parameters are found in the $K'_6 = 10^{-3}$ row in Table 1.

18 M. The corresponding range for k_{-6} is from 6.3×10^7 to 6.0×10^{13} s^{-1}. It is meaningless to consider k_{-6} values greater than the rates of bond vibrations (ca. 10^{13} s^{-1}), and therefore a lower limit to K'_6 of less than 10^{-5}, or K less than 10^{-6} M^{-1}, is imposed.

In a recent paper, Espenson and co-workers convincingly argued that equilibrium 6 lies far to the left, and kinetic considerations led to the conclusion that K_6 must be less than 10^{-3} M^{-1}.[6g] In conjunction with our simulation data, *this result narrows the possible range for K_6 to the 10^{-3}–10^{-6} M^{-1} range. The corresponding limiting values for k_6 are 10^4–10^7 $M^{-1}s^{-1}$.*

Discussion

Oxidation Potentials for the 17-Electron Radicals $CpM(CO)_3^{\bullet}$. The CV peak potentials for the chemically irreversible couples $CpCr(CO)_2(PR_3)^{\bullet/+}$ (R = Et, Ph, OMe) have been previously measured to be at least 0.9–1.4 V more positive than the electrode potentials for the reversible $CpCr(CO)_2(PR_3)^{-/\bullet}$ couples.[7g] Similarly, for the persistent radicals $TpM(CO)_3^{\bullet}$ and $Tp'M(CO)_3^{\bullet}$ (M = Cr, Mo, W),[9,10] the corresponding potential differences were in the range 0.8–0.9 V.[11] Thus, for these relatively stable radicals, radical oxidation is more difficult than oxidation of the corresponding anions by ca. 1 V (96 kJ/mol).

Due to the short-lived nature of $CpM(CO)_3^{\bullet}$ (M = Mo, W), their oxidation potentials cannot be directly measured with CV techniques at moderate sweep rates. However, it is unlikely that the differences in oxidation potentials for the Mo and W anion/neutral and neutral/cation couples are much different from the differences in the Cr systems. IR ν_{CO} frequencies are a sensitive probe for the electron density at a metal center; differences between the ν_{CO} bands for the anions[17] and radicals[18a] for the three metals are rather similar and provide additional support for this view.

The solvates $CpM(CO)_3(NCMe)^+$ (M = Mo, W) are irreversibly reduced with CV peak potentials ca. 0.3–0.5 V more negative than the anion/radical couples. The chemical irreversibility arises from rapid loss of acetonitrile from the 19-electron radicals $CpM(CO)_3(NCMe)^{\bullet}$.

Overall, these considerations lead to the conclusion that *$CpM(CO)_3(NCMe)^{\bullet}$ (M = Mo, W) are better reducing agents than $CpM(CO)_3^{\bullet}$ by ca. 1.4 V or more.*[19a] The simulations have shown that it is this situation, coupled with a sufficiently favored and rapidly established 17/19-electron equilibrium between the two, that causes the facile oxidation of $CpMo(CO)_3^-$ and $CpW(CO)_3^-$ to the cationic species. When $CpCr(CO)_3^-$ does give the cation not by this mechanism but rather by a direct oxidation at much higher potentials, this suggests that the 17/19-electron equilibrium is much less favorable, kinetically and/or thermodynamically, for Cr than for Mo and W. This is qualitatively in agreement with the less pronounced tendency of Cr complexes to undergo coordination-sphere expansion than Mo and W analogues.[19b,20]

Kinetics of Homogeneous Electron-Transfer Reactions of $CpW(CO)_3^{\bullet}$ and $CpW(CO)_3(NCMe)^{\bullet}$. The conclusion just presented has important consequences regarding the nature of the species that are homogeneously oxidized by Cp_2Fe^+ to give the cationic products $CpW(CO)_3(NCMe)^+$. For example, approximating $E(CpW(CO)_3^{\bullet/+})$ as +0.4 V vs Fc and $E(CpW(CO)_3(NCMe)^{\bullet/+})$ as −1.0 V vs Fc, the electron-transfer equilibrium constants for eqs 10 and 11 can be calculated as 1.3×10^{-7} and 1.8×10^{17}, respectively.

$$CpW(CO)_3^{\bullet} + MeCN \underset{k_{-6}}{\overset{k_6}{\rightleftharpoons}} CpW(CO)_3(NCMe)^{\bullet} \quad (6)$$

$$CpW(CO)_3^{\bullet} + Cp_2Fe^+ \underset{k_{-10}}{\overset{k_{10}}{\rightleftharpoons}} CpW(CO)_3^+ + Cp_2Fe \quad (10)$$

$$CpW(CO)_3(NCMe)^{\bullet} + Cp_2Fe^+ \underset{k_{-11}}{\overset{k_{11}}{\rightleftharpoons}} CpW(CO)_3(NCMe)^+ + Cp_2Fe \quad (11)$$

A *maximum* attainable forward rate constant for reaction 10 of about 4×10^3 M^{-1} s^{-1} is obtained by assuming that the reverse reaction proceeds at the diffusion-controlled rate ($k_{-10} = 3 \times 10^{10}$ M^{-1} s^{-1} [3e]). This upper limit to k_{10} conflicts with the observed rate constant $k_{obs} = 1.9 \times 10^7$ M^{-1} s^{-1} for the reaction between laser flash photolysis generated $CpW(CO)_3^{\bullet}$ and Cp_2Fe^+ in acetonitrile at 23 °C. The thermodynamics of the electron transfer dictate that $CpW(CO)_3(NCMe)^+$ cannot be produced via a direct electron transfer (eq 10) at this rate.

However, even a very small equilibrium constant for eq 6 will provide sufficiently high concentrations of $CpW(CO)_3(NCMe)^{\bullet}$ for it to be kinetically of greater importance than $CpW(CO)_3^{\bullet}$ as a reductant toward Cp_2Fe^+. The relationship between the equilibrium constant K_6 and the observed rate constant k_{obs} for electron transfer to Cp_2Fe^+ is $k_{obs} = k_{11}K_6[MeCN]$. The highly exergonic forward reaction (11) is likely to proceed at the diffusion-controlled rate ($k_{11} = 3 \times 10^{10}$ M^{-1} s^{-1}). Using the reported value for $k_{obs} = 1.9 \times 10^7$ M^{-1} s^{-1}, one calculates $K_6 = k_{obs}/\{k_{11}[MeCN]\} = 3.5 \times 10^{-5}$ M^{-1}, which is in the range suggested by the simulations. This binding constant is significantly lower than the ones reported for the coordination of PPh_3 (6 M^{-1}) and pyridine (0.16 M^{-1}) at $CpW(CO)_3^{\bullet}$.[6g] Since, for W, the simulations indicated that $K_6k_6 = 25$ $M^{-2}s^{-1}$, the rate of association of MeCN at $CpW(CO)_3^{\bullet}$ is obtained as $k_6 = 7 \times 10^5$ M^{-1} s^{-1}, and the rate of MeCN dissociation from $CpW(CO)_3(NCMe)^{\bullet}$ is $k_{-6} = 2 \times 10^{10}$ s^{-1}. In comparison, constants for MeCN and $(BuO)_3P$ binding at (η^6-mesitylene)$W(CO)_3^{\bullet+}$ are 0.1 and 3×10^3 M^{-1}; association rates 10^5 and 10^7 M^{-1} s^{-1}; dissociation rates 10^6 and 3×10^3 s^{-1}.

In a recent paper, Pugh and Meyer[6f] demonstrated that $CpMo(CO)_3^{\bullet}$ is unstable toward disproportionation in acetonitrile by 0.49 V (47 kJ/mol). Yet, it has been demonstrated that this

(17) IR data for $CpM(CO)_3^-$ in acetonitrile from ref 11: M = Cr, 1768, 1888 cm^{-1}; Mo, 1770, 1891 cm^{-1}; W, 1765, 1886 cm^{-1}.

(18) (a) IR data for $CpM(CO)_3^{\bullet}$ (CO matrix): Cr, 1986, 1910, 1902 cm^{-1};[18b] Mo, 2009, 1915, 1908 cm^{-1};[18c] W, 1999, 1900, 1897 cm^{-1}.[18c] (b) Mahmoud, K. A.; Rest, A. J.; Alt, H. G. *J. Chem. Soc., Chem. Commun.* **1983**, 1011. (c) Mahmoud, K. A.; Rest, A. J.; Alt, H. G. *J. Chem. Soc., Dalton Trans.* **1984**, 187.

(19) (a) Similar arguments show that $CpW(CO)_3(NCMe)Me^{\bullet+}$ is a better reducing agent than $CpW(CO)_3Me$ by 1.35 V.[19b] For other related cases, see ref 19c and 20. (b) Skagestad, V.; Tilset, M. *Organometallics* **1991**, *10*, 2110. (c) Therien, M. J.; Trogler, W. C. *J. Am. Chem. Soc.* **1987**, *109*, 5127.

(20) (a) Doxsee, K. M.; Grubbs, R. H.; Anson, F. C. *J. Am. Chem. Soc.* **1984**, *106*, 7819. (b) Zoski, C. G.; Sweigart, D. A.; Stone, N. J.; Rieger, P. H.; Mocellin, E.; Mann, T. F.; Mann, D. R.; Gosser, D. K.; Doeff, M. M.; Bond, A. M. *J. Am. Chem. Soc.* **1988**, *110*, 2109. (c) Zhang, Y.; Gosser, D. K.; Rieger, P. H.; Sweigart, D. A. *J. Am. Chem. Soc.* **1991**, *113*, 4062.

Scheme 3

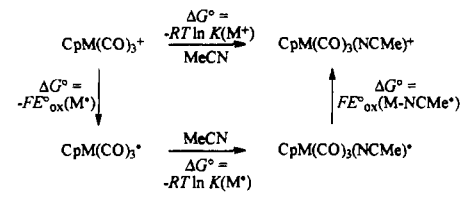

$$\ln [K(M^+)/K(M^\bullet)] = F/RT [E^\circ_{ox}(M^\bullet) - E^\circ_{ox}(M\text{-}NCMe^\bullet)] \quad (12)$$

radical disproportionation does not occur in acetonitrile.[3e] The relative rate of dimerization and disproportionation is given by $k_{dim}/\{k_9K_6[MeCN]\}$. Even the highest values allowed for K_6 based on the simulation results combined with the diffusion-controlled rate for k_9 will lead mostly to dimerization because k_{dim} is large. Oxidation of the 17-electron radical via the 19-electron radical intermediate can compete with dimerization only in the presence of oxidizing agents more potent and/or stable than $CpM(CO)_3^\bullet$. These criteria are obviously satisfied by Cp_2Fe^+ and by an electrode held at the anion oxidation potentials.

Relative Acetonitrile Affinities of $CpM(CO)_3^+$ and $CpM(CO)_3^\bullet$ in Solution. Following Breslow's seminal paper,[21] thermochemical cycles that make use of electrode potential data have been frequently used to extract quantitative data for the energetics of homolytic and heterolytic bond cleavage reactions in organic and organometallic molecules and ions.[22] Such cycles are particularly useful when transient species, for which thermochemical data cannot be obtained by more direct methods, are involved.

The thermochemical cycle in Scheme 3 may be used to estimate the relative equilibrium constants for binding of acetonitrile to $CpM(CO)_3^+$, $K(M^+)$, and $CpM(CO)_3^\bullet$, $K(M^\bullet)$. The cycle is quite similar to that employed to determine hydride affinities of organic cations and radicals.[23] The only experimental data that are needed are the oxidation potentials of $CpM(CO)_3^\bullet$, $E^\circ_{ox}(M^\bullet)$, and $CpM(CO)_3(NCMe)^\bullet$, $E^\circ_{ox}(M\text{–}NCMe^\bullet)$, both of which can be estimated as discussed already. Combination of the free-energy terms in Scheme 3 yields eq 12, which allows the determination of $K(M^+)/K(M^\bullet)$. For this analysis, we use as an estimate $E^\circ_{ox}(M^\bullet) - E^\circ_{ox}(M\text{–}NCMe^\bullet) = 1.4$ V. The available data do not allow for distinctions to be made between the magnitudes of $E^\circ_{ox}(M^\bullet) - E^\circ_{ox}(M\text{–}NCMe^\bullet)$ for the three different metals.

Taking $E^\circ_{ox}(M^\bullet) - E^\circ_{ox}(M\text{–}NCMe^\bullet) = 1.4$ V, one obtains $K(M^+)/K(M^\bullet) = 1.4 \times 10^{24}$. This number translates to a difference in bond energies of 135 kJ/mol (32 kcal/mol) for the binding of acetonitrile to $CpM(CO)_3^+$ and $CpM(CO)_3^\bullet$, respectively. The energetics of acetonitrile dissociation from the resulting 18- and 19-electron species, both of which are heterolytic bond cleavage processes in which the *ligand* retains both electrons, are therefore strongly dependent on the oxidation state, or valence electron count, of the metal. We have previously found[6d,7g,11] that the deprotonation of metal hydrides, heterolytic processes in which the *metal* retains both electrons, is greatly facilitated (by 110–140 kJ/mol) by the 1-electron oxidation of stable 18-electron hydride complexes to their 17-electron cation radicals.

Final Remarks. Available or estimated electrochemical data for the $CpM(CO)_3^-/^\bullet$ (M = Mo, W), $CpM(CO)_3^{\bullet/+}$, and $CpM(CO)_3(NCMe)^{\bullet/+}$ couples suggest that the 17-electron radicals cannot be the species that are electrochemically oxidized to give $CpM(CO)_3(NCMe)^+$ at the oxidation potentials of the anions. Digital simulations of the cyclic voltammetry response show that the radicals $CpM(CO)_3^\bullet$ are capable of reversibly binding acetonitrile with binding constants and at rates that imply the intermediacy of $CpM(CO)_3(NCMe)^\bullet$ in the oxidation process. These 19-electron radicals are kinetically competent intermediates and probably act as the true reducing agents when Cp_2Fe^+ is reduced to Cp_2Fe in the presence of $CpW(CO)_3^\bullet$ in acetonitrile.

Experimental Section

The compounds $CpM(CO)_3^-PPN^+$ (M = Cr, Mo, W) were prepared by metathesis between the sodium metalates and PPN^+Cl^- as described elsewhere,[24a] and $CpM(CO)_3(NCMe)^+PF_6^-$ (M = Mo, W) were obtained by hydride abstraction from $CpM(CO)_3H$ with $Ph_3C^+PF_6^-$ in acetonitrile.[24b]

Electrochemical Measurements. Acetonitrile and dichloromethane were distilled from P_2O_5 and CaH_2, respectively. Acetonitrile and dichloromethane containing $Bu_4N^+PF_6^-$ as the supporting electrolyte were passed through a column of active neutral alumina before use to remove water and protic impurities before electrochemical measurements. The electrolyte was freed of air by purging with purified argon, and all electrochemical measurements were carried out under a blanket of solvent-saturated argon. Electrochemical measurements were performed with an EG&G-PAR Model 273 potentiostat/galvanostat driven by an external HP 3314A sweep generator. The signals were fed to a Nicolet 310 digital oscilloscope and processed by an on-line personal computer. The working electrode was a Pt disk electrode (d = 0.6 mm), the counter electrode was a Pt wire, and the Ag wire reference electrode assembly[25] was filled with acetonitrile/0.01 M $AgNO_3$/0.1 M $Bu_4N^+PF_6^-$. The reference electrode was calibrated against Cp_2Fe, which is also used as the reference in this work. Positive-feedback iR compensation was employed; the separation of anodic and cathodic peaks for the Cp_2Fe oxidation was 59–61 mV. With the exception of Figure 4, the experimental voltammograms are not background subtracted. The appearance of the voltammograms was quite reproducible: Peak potentials were reproduced to ±10 mV for oxidation of the anion and ±20 mV for reduction of the product cation when independent measurements were performed on separate solutions. The intensity and shape of the anodic peak were largely unaffected, whereas the cathodic peak was affected (±20% intensity variations) depending on the electrode history (washing and polishing).

Acknowledgment. We acknowledge generous support from Statoil under the VISTA program, administered by the Norwegian Academy of Science and Letters.

(21) Breslow, R.; Chu, W. *J. Am. Chem. Soc.* **1973**, *95*, 411.
(22) For recent reviews, see: (a) Arnett, E. M.; Flowers, R. A., II. *Chem. Soc. Rev.* **1993**, 9. (b) Bordwell, F. G.; Zhang, X.-M. *Acc. Chem. Res.* **1993**, *26*, 510. (c) Wayner, D. D. M.; Parker, V. D. *Acc. Chem. Res.* **1993**, *26*, 287.
(23) Handoo, K. L.; Cheng, J.-P.; Parker, V. D. *J. Am. Chem. Soc.* **1993**, *115*, 5067.
(24) (a) Lai, C. K.; Feighery, W. G.; Zhen, Y.; Atwood, J. D. *Inorg. Chem.* **1989**, *28*, 3929. (b) Beck, W.; Schloter, K. *Z. Naturforsch.* **1978**, *33B*, 1214.
(25) Moe, N. S. *Anal. Chem.* **1974**, *46*, 968.